Applied Microbiology and Biotechnology (2019) 103:7231–7240
https://doi.org/10.1007/s00253-019-10001-2

ENVIRONMENTAL BIOTECHNOLOGY

Biomining of iron-containing nanoparticles from coal tailings

Danielle Maass[1] · Morgana de Medeiros Machado[2] · Beatriz Cesa Rovaris[2] · Adriano Michael Bernardin[3] · Débora de Oliveira[2] · Dachamir Hotza[2]

Received: 21 March 2019 / Revised: 23 June 2019 / Accepted: 27 June 2019 / Published online: 10 July 2019

Abstract

Sulfur minerals originating from coal mining represent an important environmental problem. Turning these wastes into value-added by-products can be an interesting alternative. Biotransformation of coal tailings into iron-containing nanoparticles using *Rhodococcus erythropolis* ATCC 4277 free cells was studied. The influence of culture conditions (stirring rate, biomass concentration, and coal tailings ratio) in the particle size was investigated using a 2^3 full factorial design. Statistical analysis revealed that higher concentrations of biomass produced larger sized particles. Conversely, a more intense stirring rate of the culture medium and a higher coal tailings ratio (% *w*/*w*) led to the synthesis of smaller particles. Thus, the culture conditions that produced smaller particles (< 50 nm) were 0.5 abs of normalized biomass concentration, 150 rpm of stirring rate, and 2.5% *w*/*w* of coal tailings ratio. Composition analyses showed that the biosynthesized nanoparticles are formed by iron sulfate. Conversion ratio of the coal tailings into iron-containing nanoparticles reached 19%. The proposed biosynthesis process, using *R. erythropolis* ATCC 4277 free cells, seems to be a new and environmentally friendly alternative for sulfur minerals reuse.

Keywords Biomining · Coal tailings · Iron sulfate nanoparticle · *Rhodococcus erythropolis* · Sulfur minerals

Introduction

Mineral coal is a complex and varied blend of organic components. Its quality, determined by the carbon content, varies according to the type and stage of the organic components. In terms of participation in the worldwide energy matrix, coal is currently responsible for about 7.9% of all energy consumption and 39.1% of all electricity generated (IEA 2017). Moreover, its share in global primary energy production, which considers other uses than electric power generation, is 26%. It is projected that this ore will maintain a similar percentage in the next 30 years, despite the increasing use and development of renewable sources such as solar, wind, and biomass energy (IEA 2017).

The solid residues generated during the cleaning and extraction processes are responsible for the main environmental impacts associated with the coal processing (Evangelou 1995; Oliveira et al. 2016). In the European Union, mining and quarrying contribute with 727 million tons of waste, representing 28.3% of the total amount of it (EUROSTAT, n.d.). Some of these residues are inert and therefore are not likely to have a significant impact on the environment. However, other fractions, especially tailings from the processing of sulfide minerals such as pyrite (FeS_2), may cause environmental and ecological risks due to their oxidation tendency in the presence of water or air. The presence of sulfur compounds favors the occurrence of metal acid leaching, which contaminates water with bioaccumulative metals, rendering it unsuitable for domestic and agricultural use (Klein and Hurlbut, 1993; Evangelou 1995).

Traditional metal recovery processes from tailings are known as pyrometallurgy and hydrometallurgy. Pyrometallurgy is the most widely used method, where the extraction and refining of metals occur through chemical reactions carried out at high temperatures (above 400 °C). Burning is the most common process to dispose of organic

✉ Danielle Maass
danielle.maass@unifesp.br

[1] Institute of Science and Technology (ICT), Federal University of São Paulo (UNIFESP), São José dos Campos, SP 12231-280, Brazil

[2] Department of Chemical and Food Engineering (EQA), Federal University of Santa Catarina (UFSC), Florianópolis, SC 88040-900, Brazil

[3] Department of Materials Engineering (PPGCEM), Universidade do Extremo Sul de Santa Catarina (UNESC), Criciúma, SC 88806-000, Brazil

materials present in coal tailings. The fusion of a crude metal concentrate generates impure metal alloys, which can be refined electrolytically. However, this method requires large amounts of energy and can form uncontrolled harmful products, while only achieving a partial separation of the metals (Guo et al. 2009). In the hydrometallurgical process, the metals are recovered using acidic and basic solutions to dissolve the solid material with subsequent precipitation of the dissolved metals. Thus, hydrometallurgy may have environmental impacts due to the presence of heavy metals in liquid effluents and the low chemical stability of the solid waste generated (Xie et al. 2015). Recently, some environmentally friendly processes have been studied to replace traditional recycling/recovering processes. One of these possible alternatives is biomining, which is a generic term to describe technologies that use biological systems (mostly prokaryotic microorganisms) to facilitate the extraction and recovery of metals present in ores or wastes (Johnson 2014). High energy costs and the growing movement towards sustainable mining have contributed significantly to the appeal of biomining, since the processes involved in this technology are often of lower costs, simpler, and easier to operate compared to conventional extractive processes (Brierley and Brierley 2013).

Several studies show that the bacteria *Actinobacter* sp. (Bharde et al. 2005), *Aquaspirillum magnetotacticum* (Narayanan and Sakthivel 2010), *Geobacter metallireducens* GS-15 (Lovley et al. 1993), *Magnetospirillum magnetotacticum* (Lee et al. 2004), *M. gryphiswaldense* (Lang and Schüler 2006), and *Thermoanaerobacter ethanolicus* TOR-39 (Roh et al. 2002) are able to recover iron from tailings and to synthesize them into iron NPs. To the best of our knowledge, the bacterium *Rhodococcus erythropolis* has been slightly used in biomining (Maass et al. 2019).

Rhodococcus sp. has remarkable characteristics such as broad catabolic diversity, unique enzymatic capabilities, and the ability to adapt under extreme conditions (Todescato et al. 2017). However, the most interesting feature in this case is its desulfurizing capacity. Recently, this strain has been used in the biodesulfurization of fossil fuels (Bachmann et al. 2014). Since *Rhodococcus* sp. is able to produce sulfate reductase enzymes and to promote the sulfur separation of recalcitrant compounds (Gupta et al. 2005), this strain can be useful in the biomining of iron from sulfur minerals.

Usually, sulfur minerals are used in the production of sulfuric acid. Emerging technologies have sought to obtain other by-products from pyrite such as coagulants, pigments, magnetite, and ferrous sulfate (Oliveira et al. 2016). Some authors studied the use of pyrite as a raw material in cement production (Alp et al. 2009) and as a catalyst in the electro-Fenton process (Labiadh et al. 2015; Barhoumi et al. 2016). Sulfur minerals have also been used as adsorbents for toxic metals, mainly due to their unusual surface properties that provide the adsorption of metal ions in a very similar form to those obtained in the oxide surface (Borah and Senapati 2006; Peng et al. 2017; Boente et al. 2018). However, the use of sulfur minerals as a precursor in the biomining of iron and in the biosynthesis of iron-containing nanoparticles (NPs) has been slightly explored (Maass et al. 2019).

Nanoscale iron particles represent a new generation of environmental remediation technologies that can provide low-cost solutions to some of the most challenging environmental cleanup problems. Iron NPs have large surface areas and high surface reactivity (Zhang 2003; Choi et al. 2018). They also offer tremendous flexibility for *in situ* applications such as the recovery of precious metals from mining industry waste and metal leachate in the areas of bioremediation, biomineralization, bioleaching, and bio-corrosion, as catalysts in various chemical reactions (Narayanan and Sakthivel 2010; Krishnamurthy et al. 2014). Some iron NPs can be coated with different surface modifying agents to better control their reactivity and mobility; they may be functionalized specifically to capture some types of molecules, or they might be supported on other materials to reduce their losses and prevent possible contamination (Gong et al. 2017; Peng et al. 2017).

Based on the above mentioned aspects, this work evaluates the synthesis of iron-containing NPs from coal tailings by *Rhodococcus erythropolis* ATCC 4277 free cells. The effects of culture conditions on the particle size were studied through a full factorial design (FFD). The NPs were characterized by transmission electron microscopy, energy dispersive spectroscopy, Fourier transform infrared spectroscopy, X-ray diffraction, and Mössbauer spectroscopy.

Material and methods

Coal tailings

Rio Deserto Mining Company Ltd. (Criciúma, Brazil) kindly provided the coal tailings. The coal tailings were a sulfur mineral that came from a coal tailing pile. The sulfur mineral was milled, sieved, and used in the granulometry range of 100–200 mesh.

Microorganism

The bacteria *Rhodococcus erythropolis* ATCC 4277 used in this study was acquired from the Tropical Culture Collection (CCT) of the "André Tosello" Research & Technology Foundation (Campinas, Brazil). As per supplier recommendation, the cells were maintained at 4 °C on Petri dishes with solid *Streptomyces* medium (SM) containing 4.0 g L^{-1} of yeast extract, 10.0 g L^{-1} of malt extract, 4.0 g L^{-1} of glucose, 2.0 g L^{-1} of calcium carbonate, and 12.0 g L^{-1} of agar.

Pre-culture

The pre-culture of *R. erythropolis* ATCC 4277 was prepared by transferring a loopful of culture from a Petri dish to flasks containing 100 mL of a sterilized nutrient medium with the following composition: 6.15 g L^{-1} of yeast extract, 5.0 g L^{-1} of malt extract, 2.0 g L^{-1} of glucose, and 1.16 g L^{-1} of calcium carbonate (Todescato et al. 2017). Afterwards, it was incubated for 24 h at 180 rpm and 24 °C.

Biomining of iron-containing nanoparticles

The biomining of iron-containing nanoparticles was studied by modifying the sulfur mineral concentration as well as the cultivation conditions. Full factorial design (FFD) permits the identification of the culture conditions that present a significant influence in the particle size. Therefore, a 2^3 FFD was realized using a fraction of sulfur mineral, stirring rate, and biomass concentration as independent variables (Table 1). Statistical analysis of the FFD was carried out using dedicated software (Statistica® 7.0). To estimate the effects, a significance level (α) of 5% was considered.

Each experiment was carried out at 30 °C in 250-mL Erlenmeyer flasks with 100 mL of the same nutrient medium used in the pre-culture for 72 h. The pH of the medium was adjusted to 7.0 prior to sterilization at 121 °C for 15 min. The pre-culture, which was previously standardized by adjusting its absorbance at 600 nm to 0.8, 0.5, or 0.2, was added to the culture medium in a concentration of 5% (*v*/*v*). Control tests were performed with the same nutrient medium described above, but without *R. erythropolis* cells. The broth medium was lyophilized for 48 h using a freeze dryer (Liotop L101, Liobras).

Table 1 Particle size obtained for fractional-designed runs

Run	Coal tailings		Biomass		Stirring rate		Particle size (nm)
	% *w*/*w*	Level	abs	Level	rpm	Level	
1	1.0	− 1	0.2	− 1	100	− 1	240.3
2	4.0	+ 1	0.2	− 1	100	− 1	48.1
3	1.0	− 1	0.8	+ 1	100	− 1	518.0
4	4.0	+ 1	0.8	+ 1	100	− 1	413.0
5	1.0	− 1	0.2	− 1	200	+ 1	132.6
6	4.0	+ 1	0.2	− 1	200	+ 1	161.4
7	1.0	− 1	0.8	+ 1	200	+ 1	251.0
8	4.0	+ 1	0.8	+ 1	200	+ 1	378.0
9	2.5	0	0.5	0	150	0	49.1
10	2.5	0	0.5	0	150	0	45.9

Characterization of iron-containing nanoparticles

Dynamic light scattering (DLS, NANO-flex, Microtrac S3000/S3500, Particle Metrix) was used to measure the size distribution of the iron-containing NPs. The stability of iron-containing NPs was determined by zeta potential analysis (Stabino Control 2.00.23, Particle Metrix). The transmission electron microscopy (TEM) analysis was carried out at an accelerating voltage of 100 kV for low-resolution imaging (JEM-1011, JEOL), after submitting the lyophilized samples to sonication for 30 min and drop it into a carbon-coated TEM grid. The samples for energy dispersive spectroscopy (EDS) analysis were coated on a double-sided carbon tape attached to the grid surface. EDS was accomplished coupled to a scanning electron microscope (SEM) (TM3030, Hitachi). The Fourier transform infrared spectroscopy (Prestige-21 FTIR, Shimadzu) analysis were carried out with a diffuse reflectance mode attachment (DRS-8400) and using a wavenumber range of 400–4,000 cm^{-1} at a resolution of 4 cm^{-1}. X-ray diffraction (XRD) measurements were used to identify the crystalline phase of the iron-containing NPs (XRD 6000, Shimadzu). The lyophilized samples were top loaded into 2.5-cm diameter circular cavity holders and run on θ/θ geometry. The diffraction pattern was recorded between 20 and 80° (2θ) with the diffractometer operating at a voltage of 20 kV and a current of 25 mA with CuKα (λ = 15,406 Å) radiation. Chemical composition of coal tailings before and after the biosynthesis was identified by energy-dispersive X-ray spectrometry (EDX-7000, Shimadzu) with an attached silicon drift detector (SDD). ^{57}Fe Mössbauer spectroscopy was accomplished to determine the hyperfine analysis. The discrete Gaussian lines were adjusted for each hyperfine site in order to obtain isomeric displacement values related to the pure metallic iron. Measurements were carried out using a standard spectrometer at room temperature, with ^{57}Co radioactive source dissolved in Rh matrix.

Results

Biomining capacity of *Rhodococcus erythropolis*

Extensive literature review revealed that rhodococci has been slightly explored to biomining processes and to the synthesis of metal NPs (Kundu et al. 2014; Maass et al. 2019). The biomining of iron from coal tailings by the bacterium *R. erythropolis* ATCC 4277 was studied under different culture conditions. Apparently, *R. erythropolis* ATCC 4277 free cells were capable not just to recover the iron from coal tailings (sulfur mineral), but also to transform it into iron NPs. The TEM analysis of the samples after biomining showed the presence of particles smaller than 50 nm (Fig. 1a). This result

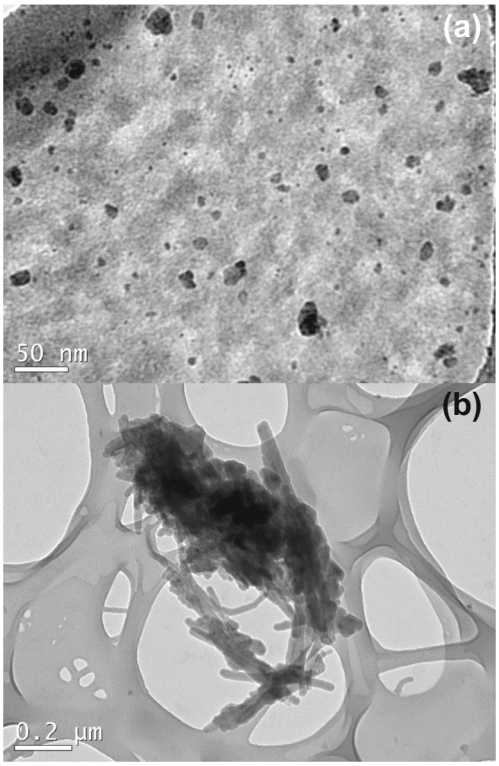

Fig. 1 TEM of *R. erythropolis* ATCC 4277 cells in the biomining culture medium (**a**) and of the iron-containing NPs biosynthesized from the coal tailings (**b**)

confirms the DLS analysis, where particles smaller than 50 nm were also determined.

Although *R. erythropolis* ATCC 4277 was capable to recover a fraction of the iron present in the coal tailings, it was observed that the recovery could be higher. One of the factors that may have influenced the biomining capacity of *R. erythropolis* ATCC 4277 was cell non-viability. TEM analyses revealed that the bacteria cells were biogranulated (Fig. 1b). Biogranulation occurs when electrostatic repulsion is overcome by van der Waals forces or hydrophobic interactions (De Carvalho et al. 2009).

Influence of culture conditions on sulfur mineral biomining

The rate and efficiency of metal sulfides biomining depend greatly on physicochemical, microbiological, and mineralogical factors (Mahmoud et al. 2017). A FFD (2^3) was accomplished to evaluate the influence of sulfur mineral fraction, stirring rate, and biomass concentration on biomining capacity and nanoparticle formation. The particle sizes obtained for each run are presented in Table 1. Nanometric particles (< 100 nm) were reached in the runs 2, 9, and 10. According to FFD results, the best conditions for iron-containing NPs formation were 2.5 %(*w*/*w*) of coal tailings, 150 rpm of stirring rate, and 0.5 abs of normalized biomass.

The factors were statistically analyzed using a significance level (α) of 5%. Tables 2 and 3 present the results of the analysis of variance (ANOVA) and the effects estimated, respectively. The most prominent effect on the particle size was related to biomass concentration (2), although all factors were found to be statistically significant.

ANOVA was also used to evaluate the predictive capacity of the model generated. Figure 2 presented the predicted versus observed values, where it is possible to observe that predicted points are slightly offset from the straight line. This means that the explained variance was 69.23% for a maximum explainable variation of 95%.

Characterization of biosynthesized iron-containing nanoparticles

In order to verify the chemical composition of the NPs synthesized, several analyses such as EDS-SEM, EDX, FTIR, XRD, TEM, and Mössbauer were accomplished. These characterization analyses were performed with samples obtained using the best culture conditions for iron NPs formation (Table 1).

EDX was used to determine the chemical composition of the sulfur mineral before and after biomining process (Table 4). The presence of S and Fe in a very expressive quantity can be associated with the presence of sulfur minerals, which are the base of pyritic residues. Pure pyrite (FeS_2) has a theoretical iron content of 46.5 wt%, so it is possible to notice that the concentration of Fe in the coal tailings before (17.98 wt%) and after the biosynthesis (11.83 wt%) is lower than the theoretical content, which indicates that the coal tailings used in this work are composed of other materials than just pyrite. EDX analysis also showed that the P element was decreased from 0.826 to 0.091 (wt%) after biomining process (see Table 4).

The chemical composition of coal tailings before and after biomining process became clearer with the results of XRD analyses, as shown in Fig. 3. Before the biomining process, the coal tailings was formed by rhomboclase ($FeH(SO_4)_2 \cdot 4H_2O$) (JCPDS 00-027-0245). Conversely, XRD analysis of the sulfur mineral after biomining (Fig. 3b) indicated the presence of potassium aluminum silicate (JCPDS 32-0731), calcium oxide (JCPDS 37-1497), and lithium chloride nitride (JCPDS 24-0605).

FTIR spectra of the coal tailings before being submitted to biomining are presented in Fig. 4. The small peaks at 490, 590, and 671 cm^{-1} are characteristic of S–S bonds, generally associated with iron disulfides (Coates 2006; Oliveira et al. 2016). The peak at 1000 cm^{-1} can be attributed to M–OH type bonds, where M is a transition metal. Bands in the range of 900 to 1200 cm^{-1} (1000, 1065, 1142, and 1232 cm^{-1}) indicate the presence of iron sulfates (Majzlan et al. 2011). The strong and wide band centered at 3448 cm^{-1} and the peak at 1620

Table 2 ANOVA for fractional-designed runs

Factor	Square sum	Degrees of freedom	Mean square	*F* test	*p* value
(1) Coal tailings % *m*/*m*	2499.2	1	2499.2	488.13	0.028795
(2) Biomass (abs)	119462.7	1	119462.7	23332.56	0.004168
(3) Stirring rate (rpm)	10981.6	1	10981.6	2144.85	0.013744
(1) and (2)	4296.6	1	4296.6	839.19	0.021967
(1) and (3)	25651.1	1	25651.1	5009.99	0.008994
(2) and (3)	11827.2	1	11827.2	2310.00	0.013244
Lack of fit	77666.5	2	38833.2	7584.62	0.008119
Pure error	5.1	1	5.1	–	–
Total square sum	252390.2	9	–	–	–

cm^{-1} are attributed to moisture (Majzlan et al. 2011). The results of FTIR analysis corroborate what was determined by XRD, i.e., that the material is in part formed by rhomboclase and part by iron disulfides.

In FTIR analysis of the sulfur mineral after biomining process, the following transmission peaks were obtained: 603, 1120, 1199, 1633, 2075, and 3448 cm^{-1} (see Fig. 4). Generally, the peak at 603 cm^{-1} is associated with iron disulfides since it is the characteristic of S–S bonds (Coates 2006; Oliveira et al. 2016). The presence of iron sulfate is indicated by bands at 1120 and 1199 cm^{-1} (Majzlan et al. 2011), and the moisture, i.e., O–OH type bonds, is indicated by the presence of peaks at 1633 and 3448 cm^{-1}.

In order to define the NPs composition and the iron oxidation state, Mössbauer spectroscopy and SEM-EDS analyses were performed. Mössbauer parameters of the coal tailings (sulfur mineral) after biomining are listed in Table 5. Mössbauer spectroscopy showed the presence of two phases: phase (1) is compatible with pyrite (FeS_2) and phase (2) is associated with Fe^{2+}. The high values found for Δ and δ parameters of phase (2) are compatible with ferrous sulfate ($Fe_2SO_4{\cdot}nH_2O$). Authors such as Wynter et al. (2004) and Ferrow et al. (2005) also found similar values when analyzing samples of pyrite and ferrous sulfate (See Table 5). The relative area shows that there was 81 wt% of phase (1) and 19 wt% of phase (2) after the biomining (Table 5), demonstrating that only a part of the rhomboclase was transformed.

As shown in Fig. 5, chemical elements with the most abundant presence in the NPs are sulfur, iron, and oxygen. The semiquantitative mass percentage was 64% oxygen, 19% sulfur, and 15% iron (see Fig. 5b), indicating that the NPs composition really approaches to ferrous sulfate (Fe_2SO_4).

Discussion

The bacterium, *Acidithiobacillus ferrooxidans*, and the related species *At. ferridurans* and *At. ferrivorans*, has a remarkable ability to oxidize ferrous iron, elemental sulfur, and various reduced forms of sulfur, to generate both ferric iron (the main oxidant of sulfide minerals) and sulfuric acid (Barrie Johnson and Hallberg 2008; Johnson 2014). Thus, *Acidithiobacillus* sp. has been widely used in metal biomining process. *Actinobacter* sp. (Bharde et al. 2005), *Aquaspirillum magnetotacticum* (Narayanan and Sakthivel 2010), *Magnetospirillum magnetotacticum* (Lee et al. 2004), and *Magnetospirillum magnetotacticum* (Bazylinski and Frankel 2004) are able to synthesize magnetite (Fe_3O_4) NPs with sizes ranging between 10 and 120 nm.

Although *Rhodococcus* sp. is also able to promote the sulfur separation of recalcitrant compounds through sulfate reductase enzymes, the genus *Rhodococcus* has been poorly explored in this type of bioprocess. To the best of our knowledge, only one previous work studied the biomining capacity

Table 3 Effects estimated from fractional-designed runs for particle size (nm)

Factor	Effect	Pure error	Student's *t* test	*p* value*	Confidence limit (− 95%)	Confidence limit (+ 95%)
Mean/intersection	223.74	0.715	312.686	0.00204	214.648	232.832
(1) Coal tailings % m/m	− 35.35	1.600	− 22.094	0.02879	− 55.680	− 15.020
(2) Biomass (abs)	244.40	1.600	152.750	0.00417	224.070	264.730
(3) Stirring rate (rpm)	− 74.10	1.600	− 46.312	0.01374	− 94.430	− 53.770
(1) and (2)	46.35	1.600	28.969	0.02197	26.020	66.680
(1) and (3)	113.25	1.600	70.781	0.00899	92.920	133.580
(2) and (3)	− 76.90	1.600	− 48.062	0.01324	− 97.230	− 56.570

*Significant at $p < 0.05$

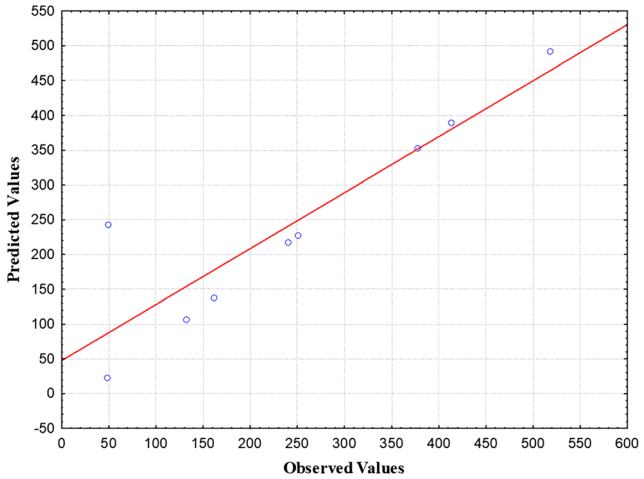

Fig. 2 Values predicted by the polynomial model *versus* experimentally observed for iron-containing nanoparticle biosynthesis as a function of particle size (nm) response

of *R. erythropolis* (Maass et al. 2019), and just one study about its ability to synthesized metal NPs (Kundu et al. 2014). The bacterium *R. erythropolis* ATCC 4277 was found to be able to recover iron from coal tailings and to transform it into ferrous sulfate nanoparticles. The biotransformation of coal tailings into high added value nanoparticles represents a promising alternative for the sustainability of coal mining and for treatment of coal tailings.

The best conditions for the sulfate iron NPs formation were defined through a FFD. Statistical analyses revealed that normalized biomass concentration had a negative effect in the NPs production, and the other two factors studied, i.e., coal tailings fraction and stirring rate, had a positive effect. Biomass concentration plays an important role in the synthesis of NPs and in the biomining rate. The negative effect of biomass concentration was also observed in the works of Almeida et al. (2017), Birla et al. (2013), and Husseiny et al. (2015). Apparently, a large quantity of cells is not necessary to obtain the amount of enzymes needed. Moreover, higher concentrations of biomass may decrease the pH of the reaction medium and directly affect both the production and the action of the reducing enzymes, making the produced NPs more susceptible to agglomeration due to their instability (Almeida et al. 2017).

Table 4 Chemical composition of the sulfur mineral before and after biomining

Element	wt% (before biomining)	wt% (after biomining)
As	0.005	0.004
C	58.324	71.090
Ca	–	1.366
Cs	0.206	–
Cu	0.009	0.006
Fe	17.976	11.830
K	0.095	1.014
Mn	0.029	0.019
P	0.826	0.091
Pb	0.013	0.009
S	21.754	13.959
Se	0.001	0.001
Si	0.752	0.600
Zn	0.007	0.005
Zr	0.003	0.002

As it is possible to observe in Table 3, the stirring rate had a positive effect on the formation of nanoparticles. According to Mahmoud et al. (2017), an efficient stirring system is required to provide adequate oxygen supplies to the microorganisms, to enhance the gas transfer rates, to obtain a high degree of homogeneity of the gas/liquid/solids system, and to maximize the volumetric gas mass transfer coefficient. The oxygen is a limiting factor that is responsible for slowing down the microbial growth rate and ultimately the biomining rate since it is used for the oxidation of the sulfide mineral (Mahmoud et al. 2017). The positive effect of stirring rate can also be explained by the preferentially aerobic catabolism of the *R. erythropolis*. Several authors discuss the metabolic pathway that promotes the production of sulfide reductase enzymes, demonstrating that it is performed only in the presence of oxygen (Aggarwal et al. 2012; Todescato et al. 2017). Thus, a greater stirring rate may increase the concentration of dissolved oxygen in the reaction medium. Moreover, the sulfur mineral tailings tend to be at the bottom of the reaction flask because they have a specific mass (5.02 g/cm^3) higher than that of water. Thus, the higher stirring rate could favor the contact between the biomass and the sulfur mineral and improve the possibility of NPs formation.

The increase in coal tailings concentration leads to smaller particle sizes (see Table 3). Some researchers explain that the positive effect of FeS_2 concentration is due to its ability to induce the release of the sulfate reductase enzyme by microorganisms, which may reduce the metals present in the substrate for NPs. As more substrate molecules (FeS_2) are delivered to the medium, the enzyme secretion by the microorganisms can increase proportionally to a threshold concentration, which, in this case, has not been observed (Birla et al. 2013; Husseiny et al. 2015; Almeida et al. 2017).

Chemical characterization of the coal tailings before being submitted to biomining process showed that this residue is basically composed of pyrite (FeS_2) and rhomboclase ($FeH(SO_4)_2{\cdot}4H_2O$). Rhomboclase has a typically post-mining origin, being formed by a pyrite alteration, especially in an arid climate (Webmineral 2018). EDX analysis also pointed out the presence of carbon in the coal tailings (see Table 4). Although the residues from mineral coal extraction are essentially inorganic, the presence of coal remains can occur. This would explain the high amount of carbon in the

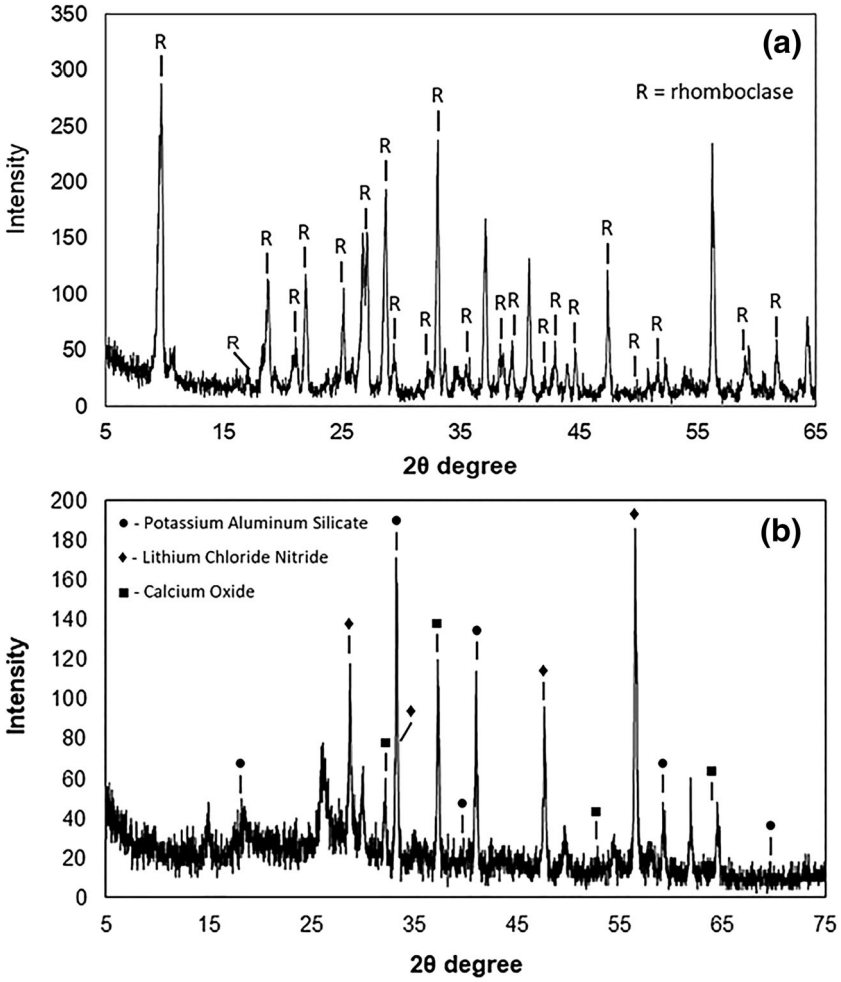

Fig. 3 XRD spectra of the coal tailings before (**a**) and after (**b**) biomining

pyrite tailings prior to biosynthesis. The decreasing of the P element concentration (wt%) after biomining process can be attributed to the formation of new bacteria cells, i.e., the P was consumed from the coal tailings to form the cell wall of new

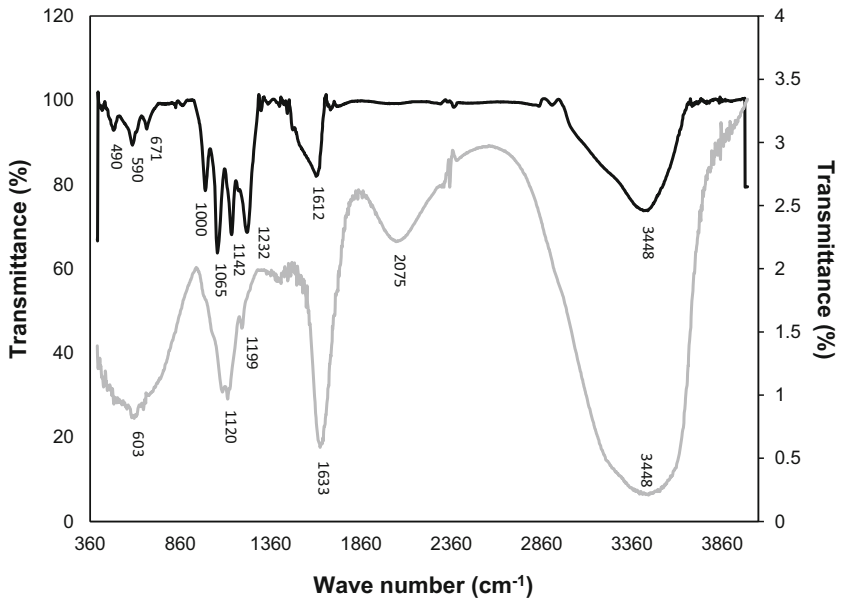

Fig. 4 FTIR spectra of the sulfur mineral before (black line (—)) and after (gray line (—)) biomining

Table 5 Mössbauer parameters for the sulfur mineral after biomining

Parameters	Phases					
	This work		(29)		(28)	
	(1)	(2)	FeS_2	$Fe_2SO_4{\cdot}nH_2O$	FeS_2	$Fe_2SO_4{\cdot}nH_2O$
Δ (mm s^{-1})	0.61	3.22	0.61	2.90	~ 0.61	~ 2.80
δ (mm s^{-1})	0.32	1.27	0.31	1.28	~ 0.31	~ 1.26
Γ (mm s^{-1})	0.30	0.40	–	–	–	–
RA (%)	81.0	19.0	–	–	–	–

δ, center shift; Δ, quadrupole splitting for the paramagnetic state; Γ, line width; SP, relative area in percentage (%)

R. erythropolis cells. According to de Carvalho et al. (2014), one of the most important characteristics of *Rhodococcus* genus cell wall is the presence of a phospholipid profile containing diphosphatidylglycerol, phosphatidylethanolamine, phosphatidylinositol, and phosphatidylinositol mannosides.

The coal tailings clearly suffered a chemical alteration after being submitted to biomining process. Chemical analyses indicated that part of the residue remained as pyrite and about 19% was transformed into ferrous sulfate (Fe_2SO_4). Only in XRD analysis was not possible to identify these compounds. The presence of those compounds could be originated from the culture medium or impurities present in the coal tailings. A poor degree of crystallization and nanometric particle sizes may have impaired the identification of the iron-containing NPs by XRD (Ferrow et al. 2005).

As described above, about 19% of the coal tailings were transformed into ferrous sulfate. The biomining capacity of *R. erythropolis* ATCC 4277 may have been impaired by cell non-viability. De Carvalho et al. (2009) affirm that growth under nutritional deprivation conditions may increase cellular hydrophobicity, which acts as an ignition force for a cell-cell junction or biogranulation. Furthermore, the resistance of this bacterium decreases with the increasing of the system toxicity, thus, making it impossible for cells to remain viable under severe conditions (De Carvalho and Da Fonseca 2004; De Carvalho et al. 2005).

Maass et al. (2019) described the biochemical mechanism behind iron NPs formation based on the Kundu et al. (2014), since the precursor used in both works are similar ($FeH(SO_4)_2{\cdot}4H_2O$ and $Zn_4(SO_4)(OH)_6{\cdot}0.5H_2O$, respectively). Although the biochemical mechanism behind the NPs formation is beyond the scope of this work, it is possible to propose a mechanism based on the works abovementioned. Thus, the formation of NPs may occur following the reaction (1). The synthesis of H_2SO_4 can be corroborated by the pH decreasing of the culture medium, since the pH went of 7.0 to 4.0 (data not shown) at the end of biomining process. However, the biochemical mechanism needs further investigation.

$$2FeH(SO_4)_2 \cdot xH2O \rightarrow Fe_2SO_4 + H_2SO_4 + xH_2O \quad (1)$$

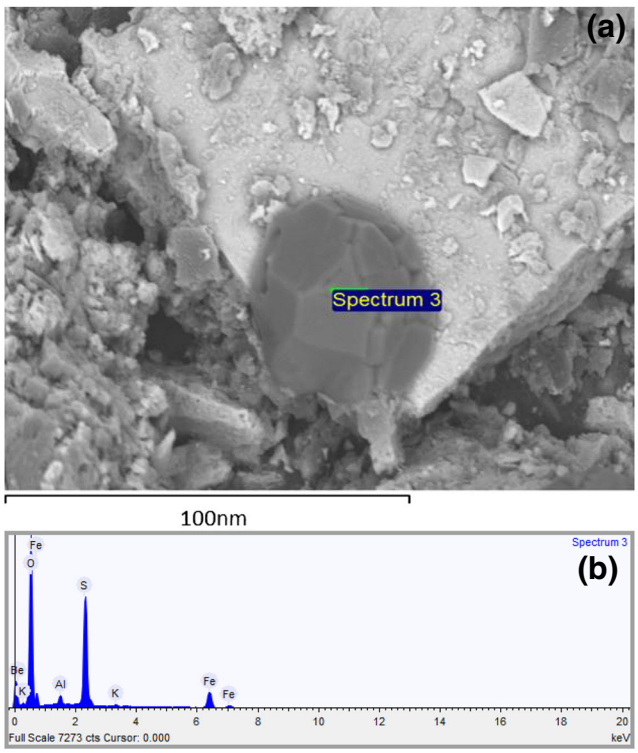

Fig. 5 SEM-EDS (**a**) and qualitative microanalysis of chemical elements (**b**) of the iron-containing NPs

Acknowledgments The authors are grateful to Prof. João Batista Marimon da Cunha of the Federal University of Rio Grande do Sul for accomplishing the Mössbauer spectroscopy analysis. We also acknowledge the LABMASSA/UFSC (Laboratório de Transferência de Massa) for the laboratorial infrastructure. Morgana M. Machado is thankful for her doctoral fellowship provided by CAPES (Coordination for the Improvement of Higher Education Personnel). Danielle Maass acknowledges her postdoctoral fellowship provided by CNPq (National Council for Scientific and Technological Development) under project number 154980/2016-1.

Funding The São Paulo Research Foundation (FAPESP) with the research grant 2019/07659-4 supports the researcher of Danielle Maass.

Compliance with Ethical Standards

Conflict of Interest The authors declare that they have no conflict of interest.

Ethical approval This article does not contain any studies with human participants or animals performed by any of the authors.

References

Almeida É, De Oliveira D, Hotza D (2017) Characterization of silver nanoparticles produced by biosynthesis mediated by *Fusarium oxysporum* under different processing conditions. Bioprocess

Biosyst Eng 40:1291–1303. https://doi.org/10.1007/s00449-017-1788-9

Aggarwal S, Karimi IA, Kilbane II JJ, Lee DP (2012) Roles of sulfite oxidoreductase and sulfite reductase in improving desulfurization by *Rhodococcus erythropolis*. Mol BioSyst 8(10):2724. https://doi.org/10.1039/c2mb25127b

Alp İ, Deveci H, Yazıcı EY, Türk T, Süngün YH (2009) Potential use of pyrite cinders as raw material in cement production: results of industrial scale trial operations. J Hazard Mater 166:144–149. https://doi.org/10.1016/J.JHAZMAT.2008.10.129

Bachmann RT, Johnson AC, Edyvean RGJ (2014) Biotechnology in the petroleum industry: an overview. Int. Biodeterior. Biodegrad. 86: 225–237

Barhoumi N, Oturan N, Olvera-Vargas H, Brillas E, Gadri A, Ammar S, Oturan MA (2016) Pyrite as a sustainable catalyst in electro-Fenton process for improving oxidation of sulfamethazine. Kinetics, mechanism and toxicity assessment. Water Res 94:52–61. https://doi.org/10.1016/J.WATRES.2016.02.042

Barrie Johnson D, Hallberg KB (2008) Carbon, iron and sulfur metabolism in acidophilic micro-organisms. In: Advances in microbial physiology. pp 201–255

Bazylinski DA, Frankel RB (2004) Magnetosome formation in prokaryotes. Nat Rev Microbiol 2:217–230. https://doi.org/10.1038/nrmicro842

Bharde A, Wani A, Shouche Y, Joy PA, Prasad BLV, Sastry M (2005) Bacterial aerobic synthesis of nanocrystalline magnetite. J Am Chem Soc. 127:9326–9327. https://doi.org/10.1021/ja0508469

Birla SS, Gaikwad SC, Gade AK, Rai MK (2013) Rapid synthesis of silver nanoparticles from *Fusarium oxysporum* by optimizing physicocultural conditions. Sci World J. 2013:1–12. https://doi.org/10.1155/2013/796018

Boente C, Sierra C, Martínez-Blanco D, Menéndez-Aguado JM, Gallego JR (2018) Nanoscale zero-valent iron-assisted soil washing for the removal of potentially toxic elements. J Hazard Mater 350:55–65. https://doi.org/10.1016/j.jhazmat.2018.02.016

Borah D, Senapati K (2006) Adsorption of Cd(II) from aqueous solution onto pyrite. Fuel. 85:1929–1934. https://doi.org/10.1016/j.fuel.2006.01.012

Brierley CL, Brierley JA (2013) Progress in bioleaching: part B: applications of microbial processes by the minerals industries. Appl Microbiol Biotechnol 97:7543–7552. https://doi.org/10.1007/s00253-013-5095-3

Choi Y, Park TJ, Lee DC, Lee SY (2018) Recombinant *Escherichia coli* as a biofactory for various single- and multi-element nanomaterials. Proc Natl Acad Sci U S A 115:5944–5949. https://doi.org/10.1073/pnas.1804543115

Coates J (2006) Interpretation of infrared spectra, a practical approach. EAC 1-18. https://doi.org/10.1002/9780470027318.a5606

De Carvalho CCCR, Da Fonseca MMR (2004) Solvent toxicity in organic-aqueous systems analysed by multivariate analysis. Bioprocess Biosyst Eng. 26:361–375. https://doi.org/10.1007/s00449-004-0381-1

De Carvalho CCCR, Parreño-Marchante B, Neumann G, Da Fonseca MMR, Heipieper HJ (2005) Adaptation of *Rhodococcus erythropolis* DCL14 to growth on n-alkanes, alcohols and terpenes. Appl Microbiol Biotechnol. 67:383–388. https://doi.org/10.1007/s00253-004-1750-z

De Carvalho CCCR, Wick LY, Heipieper HJ (2009) Cell wall adaptations of planktonic and biofilm *Rhodococcus erythropolis* cells to growth on C5 to C16 n-alkane hydrocarbons. Appl Microbiol Biotechnol. 82:311–320. https://doi.org/10.1007/s00253-008-1809-3

de Carvalho CCCR, Costa SS, Fernandes P, Couto I, Viveiros M (2014) Membrane transport systems and the biodegradation potential and pathogenicity of genus *Rhodococcus*. Front Physiol 5:1–13. https://doi.org/10.3389/fphys.2014.00133

EUROSTAT (n.d.) http://ec.europa.eu/eurostat/statistics-explained/index.php/Main_Page. Accessed 6 Feb 2018

Evangelou VP (1995) Pyrite oxidation and its control: Solution chemistry, surface chemistry, Acid Mine Drainage (AMD), molecular oxidation mechanisms, microbial role, kinetics, control, ameliorates and limitations, microencapsulation. CRC 293p. https://doi.org/10.1201/9780203741641

Ferrow EA, Mannerstrand M, Sjöberg B (2005) Reaction kinetics and oxidation mechanisms of the conversion of pyrite to ferrous sulphate: a Mössbauer spectroscopy study. Hyperfine Interact 163: 109–119. https://doi.org/10.1007/s10751-005-9200-6

Gong Y, Gai L, Tang J, Fu J, Wang Q, Zeng EY (2017) Reduction of Cr(VI) in simulated groundwater by FeS-coated iron magnetic nanoparticles. Sci Total Environ. 595:743–751. https://doi.org/10.1016/j.scitotenv.2017.03.282

Guo J, Guo J, Xu Z (2009) Recycling of non-metallic fractions from waste printed circuit boards: a review. J Hazard Mater 168:567–590. https://doi.org/10.1016/J.JHAZMAT.2009.02.104

Gupta N, Roychoudhury PK, Deb JK (2005) Biotechnology of desulfurization of diesel: prospects and challenges. Appl. Microbiol. Biotechnol. 66:356–366

Husseiny SM, Salah TA, Anter HA (2015) Biosynthesis of size controlled silver nanoparticles by *Fusarium oxysporum*, their antibacterial and antitumor activities. Beni-Suef Univ J Basic Appl Sci 4:225–231. https://doi.org/10.1016/J.BJBAS.2015.07.004

IEA (2017) Coal 2017: Analysis and forecasts to 2022. IEA Publications, International Energy Agency. https://www.iea.org/Textbase/npsum/coal2017MRSsum.pdf. Accessed 10 June 2018

Johnson DB (2014) Biomining-biotechnologies for extracting and recovering metals from ores and waste materials. Curr Opin Biotechnol 30:24–31. https://doi.org/10.1016/j.copbio.2014.04.008

Klein C, Hurlbut CS (1993) Manual of mineralogy: (after James D. Dana), 21st edn. Wiley, New York, pp 1813–1895

Krishnamurthy S, Esterle A, Sharma NC, Sahi SV (2014) Yucca-derived synthesis of gold nanomaterial and their catalytic potential. Nanoscale Res Lett. 9:627. https://doi.org/10.1186/1556-276X-9-627

Kundu D, Hazra C, Chatterjee A, Chaudhari A, Mishra S (2014) Extracellular biosynthesis of zinc oxide nanoparticles using *Rhodococcus pyridinivorans* NT2: multifunctional textile finishing, biosafety evaluation and in vitro drug delivery in colon carcinoma. J Photochem Photobiol B Biol. 140:194–204. https://doi.org/10.1016/j.jphotobiol.2014.08.001

Labiadh L, Oturan MA, Panizza M, Hamadi NB, Ammar S (2015) Complete removal of AHPS synthetic dye from water using new electro-fenton oxidation catalyzed by natural pyrite as heterogeneous catalyst. J Hazard Mater 297:34–41. https://doi.org/10.1016/J.JHAZMAT.2015.04.062

Lang C, Schüler D (2006) Biogenic nanoparticles: production, characterization, and application of bacterial magnetosomes. J Phys Condens Matter. 18:S2815–S2828. https://doi.org/10.1088/0953-8984/18/38/S19

Lee H, Purdon AM, Chu V, Westervelt RM (2004) Controlled assembly of magnetic nanoparticles from magnetotactic bacteria using microelectromagnets arrays. Nano Lett. 4:995–998. https://doi.org/10.1021/nl049562x

Lovley DR, Giovannoni SJ, White DC, Champine JE, Phillips EJP, Gorby YA, Goodwin S (1993) *Geobacter metallireducens* gen. nov. sp. nov., a microorganism capable of coupling the complete oxidation of organic compounds to the reduction of iron and other metals. Arch Microbiol. 159:336–344. https://doi.org/10.1007/BF00290916

Maass D, Valério A, Lourenço LA, de Oliveira D, Hotza D (2019) Biosynthesis of iron oxide nanoparticles from mineral coal tailings in a stirred tank reactor. Hydrometallurgy 184:199–205. https://doi.org/10.1016/J.HYDROMET.2019.01.010

Mahmoud A, Cézac P, Hoadley AFA, Contamine F, D'Hugues P (2017) A review of sulfide minerals microbially assisted leaching in stirred tank reactors. Int Biodeterior Biodegrad 119:118–146. https://doi.org/10.1016/j.ibiod.2016.09.015

Majzlan J, Alpers CN, Koch CB, McCleskey RB, Myneni SCB, Neil JM (2011) Vibrational, X-ray absorption, and Mössbauer spectra of sulfate minerals from the weathered massive sulfide deposit at Iron Mountain, California. Chem Geol. 284:296–305. https://doi.org/10.1016/j.chemgeo.2011.03.008

Narayanan KB, Sakthivel N (2010) Biological synthesis of metal nanoparticles by microbes. Adv. Colloid Interface Sci. 156:1–13

Oliveira CM, Machado CM, Duarte GW, Peterson M (2016) Beneficiation of pyrite from coal mining. J Clean Prod 139:821–827. https://doi.org/10.1016/j.jclepro.2016.08.124

Peng Z, Xiong C, Wang W, Tan F, Xu Y, Wang X, Qiao X (2017) Facile modification of nanoscale zero-valent iron with high stability for Cr(VI) remediation. Sci Total Environ. 596-597:266–273. https://doi.org/10.1016/j.scitotenv.2017.04.121

Roh Y, Liu SV, Li G, Huang H, Phelps TJ, Zhou J (2002) Isolation and characterization of metal-reducing *Thermoanaerobacter* strains from deep subsurface environments of the Piceance Basin. Colorado. Appl Environ Microbiol. 68:6013–6020. https://doi.org/10.1128/AEM.68.12.6013-6020.2002

Todescato D, Maass D, Mayer DA, Vladimir Oliveira J, de Oliveira D, Ulson de Souza SMAG, Ulson de Souza AA (2017) Optimal production of a *Rhodococcus erythropolis* ATCC 4277 Biocatalyst for biodesulfurization and biodenitrogenation applications. Appl Biochem Biotechnol. 183:1375–1389. https://doi.org/10.1007/s12010-017-2505-5

Webmineral (2018) Rhomboclase. http://webmineral.com/data/Rhomboclase.shtml#.WnmeFKinHIU. Accessed 6 Feb 2018

Wynter CI, May L, Oliver FW, Hall JA, Hoffman EJ, Kumar A, Christopher L (2004) Correlation of coal calorific value and sulphur content with 57 Fe Mössbauer spectral absorption. Hyperfine Interact 153:147–152

Xie Y, Xie S, Chen X, Gui W, Yang C, Caccetta L (2015) An integrated predictive model with an on-line updating strategy for iron precipitation in zinc hydrometallurgy. Hydrometallurgy 151:62–72. https://doi.org/10.1016/J.HYDROMET.2014.11.004

Zhang WX (2003) Nanoscale iron particles for environmental remediation: an overview. J. Nanoparticle Res. 5:323–332. https://doi.org/10.1023/A:1025520116015